

Journal of Materials Chemistry C

Materials for optical, magnetic and electronic devices

Accepted Manuscript

This article can be cited before page numbers have been issued, to do this please use: C. Lubrano, O. Bettucci, G. Dijk, A. Salleo, A. Giovannitti and F. Santoro, *J. Mater. Chem. C*, 2024, DOI: 10.1039/D3TC02849F.



This is an Accepted Manuscript, which has been through the Royal Society of Chemistry peer review process and has been accepted for publication.

Accepted Manuscripts are published online shortly after acceptance, before technical editing, formatting and proof reading. Using this free service, authors can make their results available to the community, in citable form, before we publish the edited article. We will replace this Accepted Manuscript with the edited and formatted Advance Article as soon as it is available.

You can find more information about Accepted Manuscripts in the [Information for Authors](#).

Please note that technical editing may introduce minor changes to the text and/or graphics, which may alter content. The journal's standard [Terms & Conditions](#) and the [Ethical guidelines](#) still apply. In no event shall the Royal Society of Chemistry be held responsible for any errors or omissions in this Accepted Manuscript or any consequences arising from the use of any information it contains.

The impact of hydrogen peroxide production in OECTs for *in vitro* applications

Claudia Lubrano^{1,2,3‡}, Ottavia Bettucci^{3‡‡}, Gerwin Dijk⁴, Alberto Salleo⁴, Alexander Giovannitti^{‡4*}, Francesca Santoro^{*1,2,3}

¹Institute of Biological Information Processing – Bioelectronics, IBI-3, Forschungszentrum Juelich, 52428, Germany.

²Faculty of Electrical Engineering and IT, RWTH Aachen, 52074, Germany.

³Tissue Electronics, Istituto Italiano di Tecnologia, 80125, Naples, Italy.

⁴Department of Materials Science and Engineering, Stanford University, Stanford, CA, USA.

[‡]Current address: Department of Materials Science and Milano-Bicocca Solar Energy Research Center – MIB-Solar, University of Milano-Bicocca, 20125 Milano, Italy

[‡]current address: Department of Chemistry and Chemical Engineering, Chalmers University of Technology, Göteborg 412 96, Sweden

^{‡‡}equal contribution

*correspondence to: francesca.santoro@iit.it, alexander.giovannitti@chalmers.se



1 Abstract

2 Organic electrochemical transistors (OECTs) have shown great potential in bioelectronics to
3 transduce small biological signals for applications such as the electrical recording of excitable cells
4 and assessing cell barrier properties. It is imperative that operating the OECT as a biosensor does
5 not affect the biological system. However, bias voltages applied to channel materials such as the
6 conducting polymer (CP) PEDOT:PSS has been shown to induce the formation of hydrogen
7 peroxide (H_2O_2) which can disrupt the physiology of cells. In this work, we evaluated the impact
8 of H_2O_2 formation during OECT operation by comparing an oxygen-sensitive CP (PEDOT:PSS)
9 and an oxygen-stable CP (p(gPyDPP-MeOT2)). While both CPs show high biocompatibility in
10 their non-biased, resting state, we observed large differences during the operation of the
11 electrochemical device. OECTs with PEDOT:PSS produce H_2O_2 where the H_2O_2 concentration in
12 the electrolyte depends on the channel area and the time of operation. In comparison, OECTs using
13 the oxygen-stable DPP-based polymer showed no sign of H_2O_2 formation. Further investigation
14 also revealed how the proliferation rate of neuronal cells directly interfaced with such OECTs was
15 affected by the concentration of H_2O_2 . Our work demonstrated the limitations of oxygen-sensitive
16 OECT channel materials for bioelectronic applications and provides guidance for material design
17 strategies to develop safe bioelectronic devices for real-life applications.
18
19



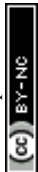
1

2 **Introduction**

3 Recent advances in the synthesis of semiconducting polymers have greatly enhanced the
4 performance of organic electrochemical transistors (OECTs).^{1,2} OECTs function in aqueous
5 electrolytes which enable the use of these devices for health monitoring and to interphase with
6 biological systems³. Moreover, OECTs have high transconductances (g_m) which enables the
7 amplification/transduction of low-voltage biological signals into electric signals^{2,4}. Examples of
8 employing OECTs for bioelectronic applications include the recording of electroactive cells,
9 impedance sensing to assess cell barrier properties, and the detection of analytes⁵⁻⁹. The OECT
10 operating mechanism is described in several recent studies and will thus not be discussed in detail
11 in this work^{10,11}. The OECT performance strongly depends on the choice of the channel material,
12 the device dimension, and the operational voltage¹².

13 Typically, the channel material consists of an organic mixed ionic-electronic conductor
14 (OMIEC)¹¹ which is designed to simultaneously transport electronic and ionic charge carriers for
15 efficient signal transduction. In contact with aqueous electrolytes, solvent molecules, and ions can
16 migrate into the bulk of the channel material (swelling) which opens the structure of the polymer
17 to enable ion penetration into the bulk of the polymer. Furthermore, upon applying an
18 electrochemical potential with respect to the gate (or reference) electrode (Ag/AgCl), electronic
19 charges are injected into the OMIEC and ions migrate from the electrolyte into the bulk of the
20 OMIEC to compensate for the electronic charges injected into the system. Conventionally, the
21 performance of OECTs is benchmarked by the product of the electronic mobility (μ) and the
22 volumetric charge storage capacitance (C^*), which are used to calculate the transconductance of
23 the transistor¹³. Although the transconductance is an important figure of merit, it only defines the
24 amplification of the device and does not include other aspects such as biocompatibility,
25 electrochemical side reactions, and operational stability. While some work described the
26 operational stability of devices¹⁴, little work has been carried out on investigating the impact of
27 electrochemical side reactions (faradaic reactions) during device operation, forming reactive side
28 products that may be harmful to biological systems.

29 Currently, PEDOT:PSS is the most used channel material as it achieves high transconductance and
30 is commercially available¹⁵. However, recent reports have demonstrated that OECTs and
31 electrodes based on PEDOT:PSS form hydrogen peroxide (H_2O_2) during operation in oxygenated



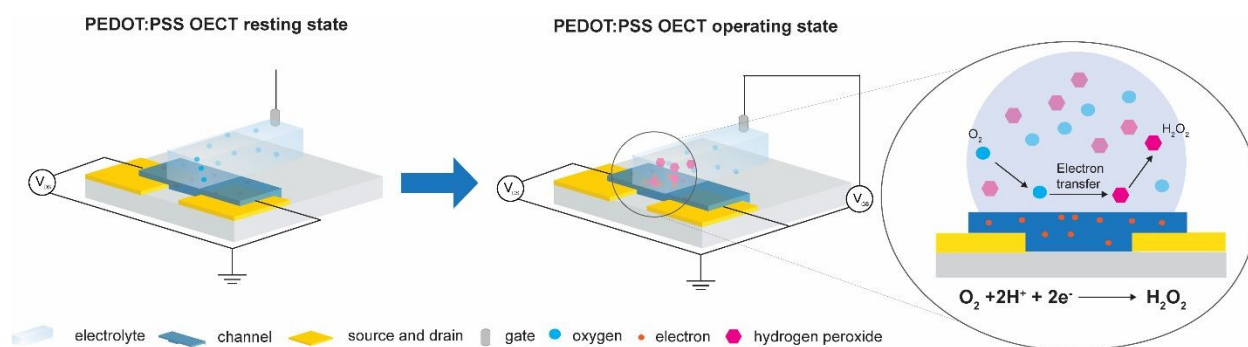
1 aqueous electrolytes^{16–20} (**Figure 1**). These electrochemical side reactions are expected to cause
2 degradation of the transistor material and importantly, also affect the health of cells that are in
3 contact with the device. H₂O₂ is a reactive oxygen species that plays an essential role in the
4 physiology of cells and tissue^{21–23}. It is generated naturally through metabolic activity and can
5 diffuse across cellular membranes to act as a molecule messenger and establish redox signaling
6 that initiates direct cellular effects such as changes in shape, proliferation, and differentiation.
7 Under normal conditions, living organisms exhibit antioxidant systems that balance the generation
8 and elimination of hydrogen peroxide. However, external factors can for instance facilitate
9 oxidative stress that disrupts the redox signaling and damages biomolecules such as DNA,
10 proteins, and lipids ultimately leading to cell death^{24–26}. Furthermore, the oxygen reduction
11 reaction (ORR) can disrupt the cell physiology and deplete oxygen in the electrolyte which may
12 lead to hypoxia for cells near the device. Thus, to engineer inert bioelectronic devices for real-life
13 applications, oxygen-stable OECT materials are needed that function without faradaic side
14 reactions with molecular oxygen to limit the accumulation of H₂O₂ during device operation.
15 In this work, we evaluated the impact of H₂O₂ formation during OECT operation in oxygen-
16 containing aqueous electrolytes by comparing an oxygen-sensitive OMIEC (PEDOT:PSS) to an
17 oxygen-stable OMIEC (p(gPyDPP-MeOT2). For each channel material, the generated H₂O₂
18 concentration was determined and the viability of neurons that were exposed to peroxide
19 containing electrolytes was examined. Furthermore, neurons cultured on a PEDOT:PSS channel
20 were visually inspected before and after OECT operation.

21 **Results and Discussion.**

23 To investigate if H₂O₂ was formed during device operation and to quantify the amount of H₂O₂
24 formed on the channel of the OECT, we prepared OECTs with a defined area and operated them
25 in ambient conditions. First, transfer curves were measured for the two different polymers (**Figure**
26 **S1**) to characterize their mode of operation. The oxygen-sensitive polymer, PEDOT:PSS, operated
27 in depletion mode where the polymer was initially in its conductive state and scanning the gate
28 potential to positive values results in reduction of the polymer, switching the device to its off state.
29 The discharged PEDOT:PSS was reactive and oxidized in the presence of molecular oxygen
30 forming H₂O₂, as illustrated in **Figure 1**. In comparison, the oxygen-stable polymer p(gPyDPP-
31 MeOT2) operated in enhancement mode. The polymer had a low electronic conductivity (device



1 begins in off state) and sweeping the gate potential to negative values induced an oxidation of the
 2 polymer that increases the electronic conductivity and switches the device to its on state. As
 3 previously reported, both the neutral and oxidized states of the polymer were not reactive towards
 4 molecular oxygen^{18,27,28}. To quantify the amount of H₂O₂ that is generated and assess the effect on
 5 cells, devices were operated by applying gate voltage pulses V_g (with fixed channel voltages, V_d)
 6 in ambient conditions, repeatedly switching the devices between the off and on state. The faradaic
 7 side reactions of the devices were then investigated by monitoring the gate current of the OEET.

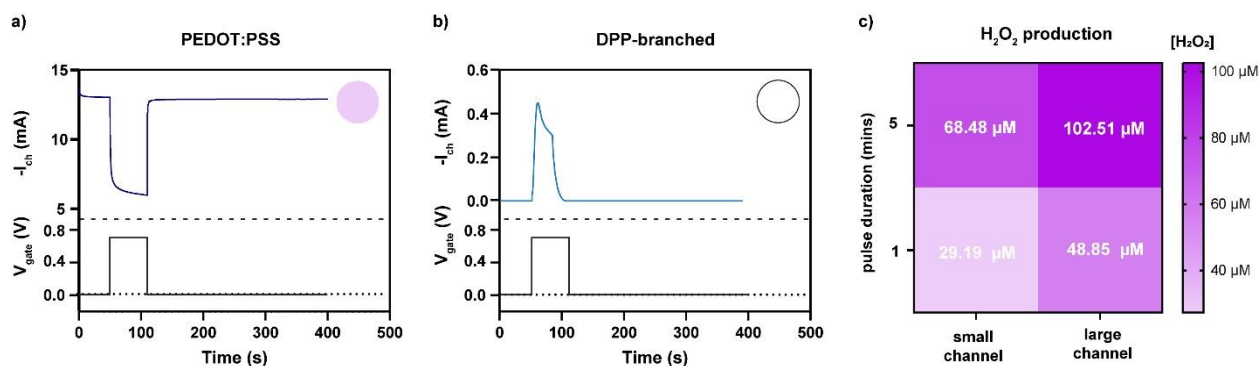


8
 9 **Figure 1.** A schematics of PEDOT:PSS OEET in its resting state and upon V_g operation, showing
 10 electron transfer from the polymer channel to the electrolyte and consequent generation of H₂O₂.

11
 12 The amount of hydrogen peroxide formation during the operation of the devices was measured
 13 with a colorimetric assay. In the presence of hydrogen peroxide, the horseradish peroxidase (HRP)
 14 catalyzed the conversion of the fluorescent probe into a colorimetric product that changed the
 15 absorbance spectra of the solution. A calibration curve was used to determine the concentration of
 16 hydrogen peroxide generated during the operation of the OEETs. (**Figure S2**). Operating the
 17 PEDOT:PSS OEET at peak g_m ($V_g = 700$ mV vs Ag/AgCl, with $V_d = -500$ mV) for 60 seconds
 18 caused generation of H₂O₂ in the electrolyte ranging from 20 to 50 μ M (**Figure 2a**). On the
 19 contrary, no hydrogen peroxide was detected (considering the experimental concentration limit of
 20 5 μ M) in the electrolyte of the OEET using polymer p(gPyDPP-MeOT2) (**Figure 2b**). For the
 21 PEDOT:PSS OEETs, the concentration of generated H₂O₂ was determined for different durations
 22 of the applied gate potential as well as for different channel dimensions. OEETs with millimeter
 23 and micrometer scale dimensions were operated for 1 and 5 minutes and the colorimetric assay
 24 was used to determine the H₂O₂ concentration (color map in **Figure 2c**). We observed the highest
 25 concentration of H₂O₂ for the large OEET (7x4 mm²) when a long gate pulse (5 minutes) was



1 applied indicating that the H_2O_2 formation depended on the active area of the device and the
 2 operation time. The number of charges injected from the gate electrode into the polymer channel
 3 correlated to the generated concentration of H_2O_2 , confirming that the by-products from the
 4 electrochemical reactions were directly related to the biasing of the OECT (**Figure S3**).

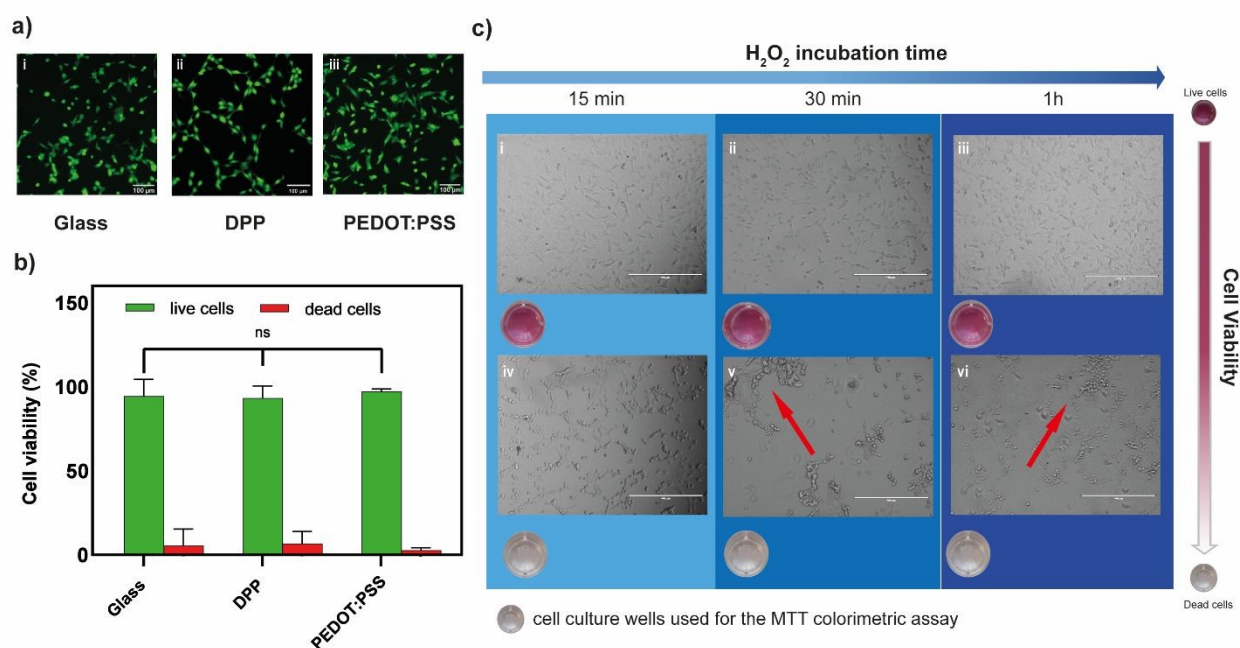


6
 7 **Figure 2.** Current response of the OECT with (a) PEDOT:PSS and (b) p(gPyDPP-MeOT2) upon
 8 applying a square voltage pulse at the gate electrode ($V_g = 700$ mV, and $V_d = -500$ mV for
 9 PEDOT:PSS, $V_g = -700$ mV, and $V_d = -100$ mV for p(gPyDPP-MeOT2)). The circular insets show
 10 the concentration of peroxide recalling the same color code reported in **Figure 3c**. Degradation of
 11 p(gPyDPP-MeOT2) is observed at potentials > -650 mV¹⁴. c) Color map representing the
 12 concentration of H_2O_2 (expressed in μM) produced during the operation of a PEDOT:PSS OECT
 13 for different channel areas and gate pulse duration.

14
 15 The biocompatibility of both polymers was first assessed in their unbiased state (*i.e.*, no gate
 16 voltage was applied), by cultivating neuronal cells (HT22) on polymer films and using a live/dead
 17 fluorescence assay. After 24 hours in culture, high percentages of green fluorescent cells (> 95
 18 %) were found indicating excellent viability on both PEDOT:PSS and p(gPyDPP-MeOT2)
 19 (**Figure 3a i-iii**). No significant difference in the percentage of live cells was found compared to
 20 the glass substrate control, suggesting negligible cytotoxic effects (**Figure 3b**). To determine
 21 whether the amount of peroxide produced during PEDOT: PSS-based OECT operation affected
 22 the cell viability, two concentrations of H_2O_2 ($20 \mu\text{M}$ and $100 \mu\text{M}$) were tested, corresponding to
 23 the amount of peroxide produced with large channel area-long pulse duration and small channel
 24 area-short pulse duration, respectively. After 1 day from plating, HT22 cells were exposed to
 25 hydrogen peroxide by exchanging the cell medium with H_2O_2 -containing medium at the desired



1 concentration after which the metabolic activity was evaluated at different time points through an
 2 MTT assay. At low H_2O_2 concentration ($20\ \mu\text{M}$), a slight decrease in the metabolic activity was
 3 observed that was proportionally related to the exposure time to H_2O_2 (**Figure S4**). Increasing the
 4 H_2O_2 concentration to $100\ \mu\text{M}$ showed a large change in the absorbance values after 15 minutes,
 5 indicating a significant decrease in the metabolic activity of cells (**Figure S4** and **Figure 3c**). This
 6 was further confirmed by a change in the cell shape as well as by the presence of cell clusters
 7 (**Figure 3c iv-vi**). These results demonstrated the sensitivity of HT22 cells hydrogen peroxide
 8 produced concentrations during the transistor operation.



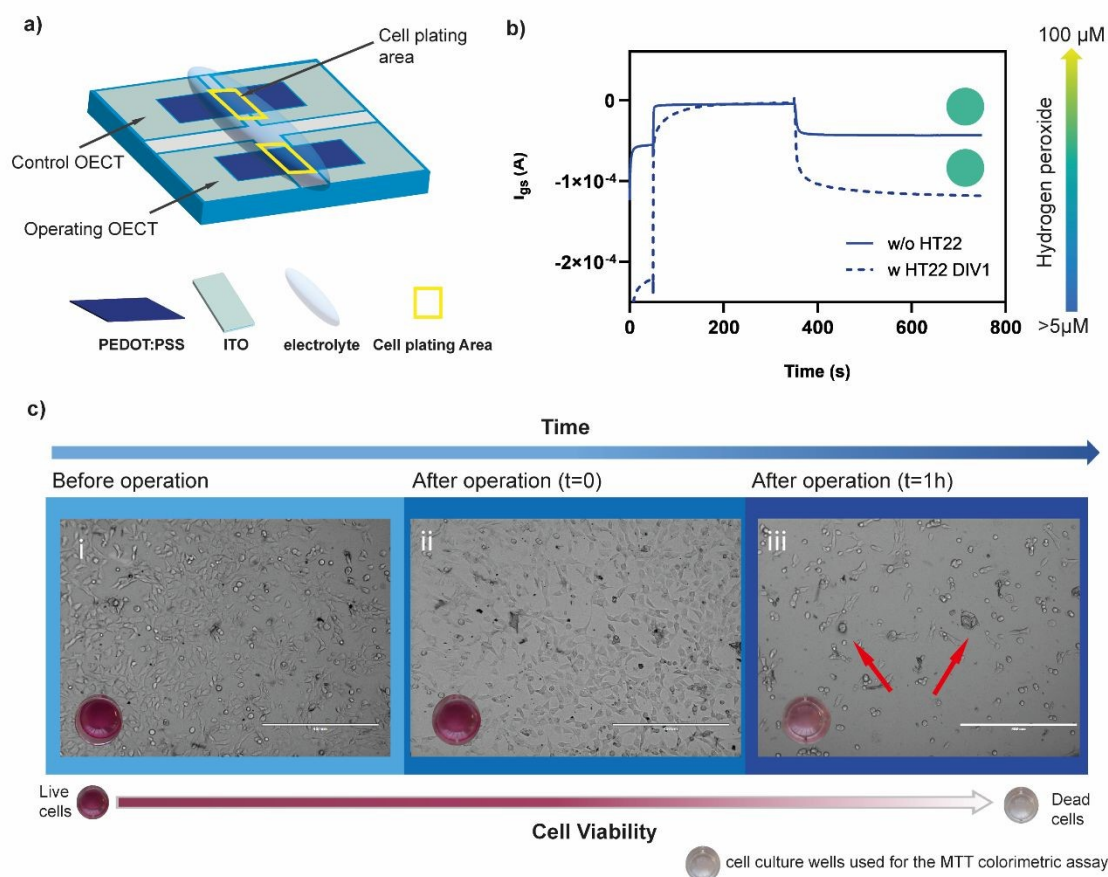
9
 10 **Figure 3.** a) HT22 cell viability ($60.000\ \text{cell}/\text{cm}^2$) assay showing fluorescently labeled live (green)
 11 and dead (red) cells on glass (i), p(gPyDPP-MeOT2) polymer (ii) and PEDOT:PSS (iii). b)
 12 Percentage of live and dead cells reported as mean \pm SEM ($n= 3$). c) Brightfield images of HT22
 13 cells seeded on glass at different time points (15, 30, and 60 min) without (i-iii) and with (iv-vi)
 14 $100\ \mu\text{M}$ H_2O_2 produced by operating the OECT. The circles are the MTT coloring indicating cell
 15 viability (pink: live cells, transparent: dead cells) and the red arrows locate cells clusters that were
 16 formed. Scale bar: $100\ \mu\text{m}$.

17
 18 To evaluate whether the presence of cells might affect the production of hydrogen peroxide
 19 protecting the polymer form undergoing the ORR, HT22 cells were cultivated ($60.000\ \text{cell}/\text{cm}^2$)



1 on top of a PEDOT:PSS OECT, covering the channel area (**Figure 4a**). The device was operated
 2 at $V_g=700$ mV and $V_d=-500$ mV for 5 minutes. Comparing the amount of H_2O_2 produced before
 3 and after cell plating, no significant difference was found ($\lambda_{570before}=0.111\pm0.011$
 4 $\lambda_{570after}=0.099\pm0.020$, $n=3$) suggesting that the presence of cells is not limiting the generation,
 5 diffusion and detection of peroxide (**Figure 4b**).

6 After device operation, cells were incubated for 1 hour in the same media. The absorbance values
 7 evaluated through MTT assay indicated a drastic decrease in the metabolic activity of the HT22
 8 ($\lambda_{570}=0.122$) with respect to the control ($\lambda_{570}=0.348$) (not operated device) (**Figure 4c**). Similar
 9 results were found with 3 different devices (**Figure S5**). Brightfield images showed round-shaped
 10 morphology and cluster formation confirming the adverse effects of oxidative stress on the cells
 11 physiology.



12 **Figure 4.** a) OECT device on a glass substrate with ITO contacts (source and drain) and two spin
 13 coated PEDOT:PSS channels. Each glass substrate contained two OECTs (cell plating area 5
 14 mm^2). One OECT was used as a control (no voltage is applied during the experiment) and the other
 15 OECT is operated (by applying 700 mV). b) Output channel current upon the application of a 5
 16



1 min square voltage pulse at the gate with and without cells (dotted and solid line, respectively). c)
2 Brightfield images of the HT22 cell line before operation (i), directly after applying the voltage
3 pulse (ii) and after 1h from applying the voltage pulse (iii). Red arrows pointing at cells clusters
4 that were formed. Scale bar: 100 μm .

5 6 **Conclusions**

7 In this work, we demonstrated the impact of hydrogen peroxide generated by OECTs on neuronal
8 cells for two distinguished OMIEC materials. Cells proliferation rate was not altered when seeded
9 on the unbiased OMIECs, showing the non-toxic nature of the OMIECs. However, when operating
10 the oxygen-sensitive OMIEC in electrochemical transistors, the production of cytotoxic hydrogen
11 peroxide was observed which significantly affected the cell viability. We observed a strong
12 correlation between the amount of hydrogen peroxide produced and the duration of the applied
13 potential as well as the channel area of the device. Importantly, operating OECTs with
14 PEDOT:PSS (channel area of 28 mm^2) formed up to 100 μM of H_2O_2 after operating the device
15 for 5 minutes, which strongly impacted the physiology of the cells. In comparison, the oxygen-
16 stable (p(gPyDPP-MeOT₂)) showed no sign of H_2O_2 formation during operation at peak
17 transconductance, paving the way for the development of safe bioelectronic devices. Future
18 materials design for OECTs should therefore not merely focus on increasing the transconductance,
19 but also consider the electrochemical reactions and resulting byproducts to support the
20 development of safer bioelectronic devices.

21 22 23 **Experimental section**

24 **Materials**

25 PEDOT:PSS was purchased from Clevios (PH 1000, Merck Life Science S.r.l., Italy). Polymer
26 p(gPyDPP-MeOT₂) based on pyridine-flanked diketopyrrolopyrrole (PyDPP) with bithiophene
27 (T₂) or 3,3'-methoxybithiophene (MeOT₂) were synthesized by a Stille polymerization as
28 previously described¹⁸.

29 30 **4.1. Large organic electrochemical transistor fabrication**



1 A two-squared patterned ITO coated glass (Surface resistivity $20 \Omega \text{ cm}^{-2}$, 25 mm x 12.5 mm,
2 Xinyan Technology Ltd., Hong Kong) was cleaned with deionized water, acetone (Merck Life
3 Science S.r.l., Italy), and 2-propanol (Merck Life Science S.r.l., Italy) (10 minutes for each solvent)
4 and dried with compressed air. Then, the ITO glass underwent a plasma activation (2 minutes, 20
5 W) to favor the spin coating of a previously prepared PEDOT:PSS aqueous solution (5 vol.%
6 ethylene glycol (Merck Life Science S.r.l., Italy), 0.002 vol.% DBSA (Merck Life Science S.r.l.,
7 Italy), and 1 vol.% GOPS (Merck Life Science S.r.l., Italy) added to a commercial Hereaus Clevios
8 PH1000) that was sonicated 30 minutes before use. The PEDOT:PSS was spin coated at 2000
9 r.p.m. for 2 minutes with an acceleration of 400 r.p.m s^{-1} and annealed 1 hour at 140°C . Finally,
10 to pattern the PEDOT:PSS channel area, a plasma etching (15 minutes, 100 W) was performed
11 covering the PEDOT strip with a Polydimethylsiloxane (PDMS) masks (15 mm x 7 mm) to form
12 a (28 mm^2 channel). Later, the OECT was left in deionized water overnight to promote the
13 PEDOT:PSS swelling.

14

15 **Small organic electrochemical transistor fabrication**

16 Interdigitated electrodes (Micrux, 15 pairs of electrodes with $W = 1950 \mu\text{m}$, $L = 10 \mu\text{m}$) were
17 cleaned by sonication for 15 minutes in acetone and isopropanol, followed by an ozone treatment
18 for 5 minutes. Devices were prepared by spin coating polymer solution. For PEDOT:PSS, the
19 above-described solution mixture was spin coated at 3000 RPM, followed by an annealing step at
20 120°C for 15 minutes. The device was rinsed with DI water and dried before testing. For polymer
21 p(gPyDPP-MeOT2), a polymer solution was prepared by dissolving the polymer in chloroform
22 (10 mg/mL). The polymer solution was filtered with a $0.45 \mu\text{m}$ filter and spin cast at 1000 RPM
23 without further thermal treatment. The area of the devices was defined by removing the polymer
24 manually with a sharp blade.

25 **OECT operation**

26 Following characterizations have been performed by using a commercial platform (ARKEO, Cicci
27 Research, Italy).

28 *Transfer-characteristic*

29 Devices were characterized by using two measurement probes connected to the source and drain
30 electrodes and a third one connected to the Ag/AgCl gate electrode. Transfer curves were taken by



1 sweeping the gate voltage from -0.8 V to 0.8 V with a scan rate of 50 mV s^{-1} and the drain voltage
2 (both versus the source potential) from -0.6 V to 0.1 V with a scan rate of 50 mV s^{-1} .

3 *Pulsed measurements*

4 Pulsed measurements on devices were performed by using the previous platform and setup,
5 keeping a fixed drain voltage of $V_{ds} = -500$ mV a voltage square pulse at the gate electrode (PW =
6 5 mins, $V_g = 700$ mV).

8 **Peroxide assay**

9 To evaluate the amount of peroxide produced during the transistor operation the Peroxidase
10 Activity Assay Kit (Merck Life Science S.r.l., Italy) has been used exploiting the capability of
11 peroxidase to catalyzes the reaction between H_2O_2 and a fluorescent probe, resulting in a
12 colorimetric (570 nm) product, proportional to the peroxidase activity present. One unit of
13 peroxidase is defined as the amount of enzyme that reduces 1.0 μ mole of H_2O_2 per minute at $37^\circ C$.
14 After operating the device, the electrolyte has been removed and developed in another vial with
15 the appropriate amount of reagent following the protocol reported in the commercial kit. The
16 solution was then measured spectrophotometrically using Dynatech MR580 Microelisa reader,
17 using a test wavelength of 570 nm.

18 **Cell culture, biocompatibility, and viability essay.**

19 *Live-dead assay*

20 The experiments were performed using HT22 cells (ATCC, Italy), an immortalized mouse
21 hippocampal cell line. HT22 cells were cultured in 25 mm² flask in DMEM:F-12 (1:1) media
22 (Merck Life Science S.r.l., Italy) supplemented with 10% fetal bovine serum (Merck Life Science
23 S.r.l., Italy), 1% penicillin/streptomycin (Merck Life Science S.r.l., Italy), 1% L-Glutamine (Merck
24 Life Science S.r.l., Italy), in a 5% CO_2 incubator at $37^\circ C$. Confluent HT22 cells were trypsinated
25 using Trypsin-EDTA 0.25% (Life Technologies Italia, Italy) and cells were seeded on the
26 polymeric substrates at a density of 79.000 cells/cm² and left in the incubator at $37^\circ C$ for 24 hours.
27 To assess the biocompatibility cells were stained with a solution of Calcein-AM (Merck Life
28 Science, final concentration $1\mu g/mL$) and Ethidium Homodimer (Thermo Fisher, final
29 concentration $10\mu g/mL$) in PBS and incubated at $37^\circ C$ for 10 minutes.

31 *MTT assay*



1 HT22 (50.000 cells/cm²) per well were seeded into a 24-well tissue culture plate for 24 hours.
2 Before plating, substrates were functionalized with poly-L-lysine (PLL, Merck Life Science S.r.l.,
3 Italy) 0.01% v/v (aqueous solution), incubated at 37 °C overnight and then washed three times
4 with PBS (Merck Life Science S.r.l., Italy). A solution of MTT (3-(4,5-dimethylthiazol-2-yl)-2,5-
5 diphenyl tetrazolium bromide (Abcam, UK) in 1x solution of PBS (Merck Life Science S.r.l.,
6 Italy) (5 mg/mL) was added to the wells (200 µL in 1 ml of medium) and incubated at 37°C for 4
7 hours. After the removal of the medium, 1 mL of DMSO (Merck Life Science S.r.l., Italy) was
8 added to all wells and mixed thoroughly to dissolve the dark blue crystals (insoluble purple
9 formazan formed by cleavage of the tetrazolium ring by dehydrogenase enzymes). After a 1 hour
10 at room temperature, to ensure that all crystals were dissolved, the DMSO solution was measured
11 spectrophotometrically using Dynatech MR580 Microelisa reader, using a test wavelength of 570
12 nm.

13

14

15 References

- 16 1 J. Rivnay, S. Inal, A. Salleo, R. M. Owens, M. Berggren and G. G. Malliaras, *Nat Rev Mater*,
17 2018, **3**, 1–14.
- 18 2 A. Spanu, L. Martines and A. Bonfiglio, *Lab on a Chip*, 2021, **21**, 795–820.
- 19 3 Z. Zhao, Z. Tian and F. Yan, *Cell Reports Physical Science*, 2023, **4**, 101673,
- 20 4 M. Sophocleous, L. Contat-Rodrigo, E. García-Breijó and J. Georgiou, *IEEE Sensors Journal*,
21 2021, **21**, 3977–4006.
- 22 5 C. Yao, Q. Li, J. Guo, F. Yan and I.-M. Hsing, *Advanced Healthcare Materials*, 2015, **4**, 528–
23 533.
- 24 6 X. Gu, S. Y. Yeung, A. Chadda, E. N. Y. Poon, K. R. Boheler and I.-M. Hsing, *Advanced*
25 *Biosystems*, 2019, **3**, 1800248.
- 26 7 L. H. Jimison, S. A. Tria, D. Khodagholy, M. Gurfinkel, E. Lanzarini, A. Hama, G. G.
27 Malliaras and R. M. Owens, *Advanced Materials*, 2012, **24**, 5919–5923.
- 28 8 A. M. Pappa, D. Ohayon, A. Giovannitti, I. P. Maria, A. Savva, I. Uguz, J. Rivnay, I.
29 McCulloch, R. M. Owens and S. Inal, *Science Advances*, 2018, **4**, eaat0911.



- 1 9 S. Han, S. Yamamoto, A. G. Polyravas and G. G. Malliaras, *Advanced Materials*, 2020, **32**,
2 2004790.
- 3 10 G. LeCroy, C. Cendra, T. J. Quill, M. Moser, R. Hallani, J. F. Ponder, K. Stone, S. D. Kang,
4 A. Y.-L. Liang, Q. Thiburce, I. McCulloch, F. C. Spano, A. Giovannitti and A. Salleo, *Mater.*
5 *Horiz.*
- 6 11 B. D. Paulsen, K. Tybrandt, E. Stavrinidou and J. Rivnay, *Nat. Mater.*, 2020, **19**, 13–26.
- 7 12 D. Ohayon, V. Druet and Sahika Inal, *Chem. Soc. Rev.*, 2023, **52**, 1001–1023
- 8 13 S. Inal, G. G. Malliaras and J. Rivnay, *Nat Commun*, 2017, **8**, 1767.
- 9 14 S. T. Keene, C. Lubrano, S. Kazemzadeh, A. Melianas, Y. Tuchman, G. Polino, P.
10 Scognamiglio, L. Cinà, A. Salleo, Y. van de Burgt and F. Santoro, *Nat Mater*, 2020, **19**, 969–
11 973.
- 12 15 M. J. Donahue, A. Sanchez-Sanchez, S. Inal, J. Qu, R. M. Owens, D. Mecerreyes, G. G.
13 Malliaras and D. C. Martin, *Materials Science and Engineering: R: Reports*, 2020, **140**,
14 100546.
- 15 16 G. Dijk, H. J. Ruigrok and R. P. O'Connor, *Advanced Materials Interfaces*, 2021, **8**, 2100214.
- 16 17 E. Mittraka, M. Gryszel, M. Vagin, M. J. Jafari, A. Singh, M. Warczak, M. Mittrakas, M.
17 Berggren, T. Ederth, I. Zozoulenko, X. Crispin and E. D. Głowacki, *Advanced Sustainable*
18 *Systems*, 2019, **3**, 1800110.
- 19 18 A. Giovannitti, R. B. Rashid, Q. Thiburce, B. D. Paulsen, C. Cendra, K. Thorley, D. Moia, J.
20 T. Mefford, D. Hanifi, D. Weiyuan, M. Moser, A. Salleo, J. Nelson, I. McCulloch and J.
21 Rivnay, *Advanced Materials*, 2020, **32**, 1908047.
- 22 19 J. Ehlich, L. Migliaccio, I. Sahalianov, M. Nikić, J. Brodský, I. Gablech, X. T. Vu, S.
23 Ingebrandt and E. D. Głowacki, *J. Neural Eng.*, 2022, **19**, 036045.
- 24 20 M. Jakešová, D. H. Apaydin, M. Sytnyk, K. Oppelt, W. Heiss, N. S. Sariciftci and E. D.
25 Głowacki, *Adv. Funct. Mater.*, 2016, **26**, 5248.
- 26 21 B. D'Autréaux and M. B. Toledano, *Nat Rev Mol Cell Biol*, 2007, **8**, 813–824.
- 27 22 H. J. Forman, M. Maiorino and F. Ursini, *Biochemistry*, 2010, **49**, 835–842.
- 28 23 K. M. Holmström and T. Finkel, *Nat Rev Mol Cell Biol*, 2014, **15**, 411–421.
- 29 24 H. Sies, *Redox Biology*, 2017, **11**, 613–619.
- 30 25 H. Sies, *Journal of Biological Chemistry*, 2014, **289**, 8735–8741.
- 31 26 V. I. Lushchak, *Chemico-Biological Interactions*, 2014, **224**, 164–175.



- 1 27 J. Nelson, *Energy Environ. Sci.*, 2023, **16**, 337–337.
- 2 28 A. D. L. F. Durán, A. Y.-L. Liang, I. Denti, H. Yu, D. Pearce, A. Marks, E. Penn, J. Treiber,
- 3 K. Weaver, L. Turaski, I. P. Maria, S. Griggs, X. Chen, A. Salleo, W. C. Chueh, J. Nelson, A.
- 4 Giovannitti and J. T. Mefford, *Energy Environ. Sci.*, 2023

